

Prediction of Quality Estimation by Supervised Learning for Electrocardiogram Noise Detection

Veerabomma Supraja^{1,2*}, Pasumarthy Nageswara Rao³, Mahendra Nanjappa Giri Prasad⁴

Submitted: 22/03/2023

Revised: 23/05/2023

Accepted: 09/06/2023

Abstract: The specificity and sensitivity of arrhythmia detection from electrocardiograms is a crucial objective in detecting pervasive computing methods. The noise is pervasive to electrocardiograms, which is since the electrocardiogram signals often transmit through distributed computing environments such as the medical internet of things (medical IOT). The noisy electrocardiograms are ubiquitous to false alarming in these distributed and pervasive computing-aided methods. The detection of noise scope in electrocardiograms is the primary objective in machine learning-based arrhythmia detection methods addressed in this manuscript. The proposed method classifies the given electrocardiograms are noisy or not. Concerning this, the method uses the electrocardiograms' temporal and spectral features. The proposed method's performance has been assessed using multifold cross-validation and scaled by comparing it with the contemporary contribution give better specifications as specificity 93.9% sensitivity 95.3%, and accuracy 94.4%.

Keywords: *Electro Cardiogram (ECG), Baseline Wandering (BA), powerline interference (PLI), Weiner Filter (WF), Fourier-transform (FT).*

1 Introduction

ECG is the commonly used cardiology test for assessing heart performance, wherein the electrical readings provide significant inputs [1]. The electrodes' key function is detecting small electrical changes resulting from the facets of repolarization, depolarization wherein the electrophysiological pattern for the heart muscles is assessed at each level of the heartbeat conditions [1]. Many distinct observations result in outcomes from the tests. For instance, there is potential scope for measuring heart rate consistency, size, and placement of the heart function conditions. Even the evaluations about the performance of any implanted devices like pacemakers or other such regulating medical devices, too, can be assessed. The graph movements indicate the heart's function during the period wherein the medical devices are used to detect the heart rates by placing the device nodes over the skin's outer surfaces and the electrodes that are being observed.

ECG (Electro Cardiogram) is the device used for garnering data as ECG signals constitute certain indicators as the common readings from the system, technically defined as

- Intervention Basic
- Interference feed line

Information garnered from the readings of ECG devices' can be very effective for measuring the abnormalities about the heart rhythms [2], [3], and more categorically in assessing the fundamental readings to guide any significant and detailed tests to be carried out [4]. As discussed in [5], the ECGs can be very resourceful for detecting damage to specific portions based on the myocardium resulting from myocardial infarctions [5]. The other important aspect is digitally collecting information and the ECG data, which shall be resourceful for handling the ECG signal analysis automatically [6]. Routine electrical line readings and the baseline drift [7] are the two distinct factors that signify the real condition of the readings from a patient record for whom the ECG records are tested. The interference power line results from streams due to the inaccuracies like the improper placement of the electrodes, unhygienic electrodes, or any loose contact over the machinery.

The interference power line is usually 50 Hz. The basal movement results in the flexible impedance resulting from electrode skin for the patient's response [8], [9]. Those two critical factors play a vital role in the clinical

¹Department of Electronics and Communication Engineering, Jawaharlal Nehru Technological University Anantapur, Anantapuramu, Andhra Pradesh - 515002, India

Email ID: suprajaece10@gmail.com

²Ravindra college of Engineering for Women, Kurnool, Affiliated to Jawaharlal Nehru Technological University Anantapur, Anantapuramu, India.

³Department of Electronics and Communication Engineering, Vardhaman College of Engineering, Anantapuramu, Andhra Pradesh - 501218, India
Email ID: nrraop@yahoo.com

⁴Professor Department of Electronics and Communication Engineering, Jawaharlal Nehru Technological University Anantapur College of Engineering, Anantapuramu, Andhra Pradesh - 515002, India.
Email ID: mahendragiri1960@gmail.com

monitoring and ECG signal masks for patients' diagnoses. Despite the scope of applying a filter is feasible for reducing the noise power (stopband notch filter), it still does not suffice the requirement in handling the scale or frequency characteristics of the noise. Considering the constraints, the optimal signal focus on non-stationary processes remains the choice for handling noise reduction. Conventional models were only successful to an extent. Certain models like the adaptive filtering procedures have been considered for canceling the non-static interference. The process wherein the noise ratio in the signals is eliminated or mitigated to the optimal extent is the Filtration [10], [11]. The other significant aspects of the filtering process are smoothing and prediction. Numerous approaches were proposed for addressing enhancements to the process using ECG adaptive and other novel range of techniques used for filtering [12]. The adaptive filtering process is generally based on the cardinal model essential for managing signals that do not require any statistical characteristics of the signal.

One of the ECG process constraints is frequent interruption due to distinct noises and other such disturbances. Earlier works have classified the interruptions [13], [14], [15] as BA (Baseline Wandering), PLI (powerline interference), and MA (Muscle Artifacts). Certain factors like the subject movements of the respiratory activities lead to BA, wherein it manifests in slow wandering baselines resulting from facets like the body movements, which could be random. ECGs constituting the impact of MAs has a critical issue of muscular contraction artifacts. PLIs lead by electrical power leakage or any other such inappropriate equipment handling conditions has a significant impact in terms of ECG amplitudes and indistinct kind set of isoelectric baseline conditions. It is imperative to address such conditions of noises leading to disturbances, as the ECG signal analysis interpretation might lead to misled or inaccurate insights for diagnosis.

Section 1 of this paper discusses the introduction of electrocardiogram and several other models. Section 2 explores the related work on electrocardiograms for noise detection. A variety of literature materials have been reviewed and showcased. Section 3 is where the methods and materials are located. In Section 4, an empiric examination is presented. This section juxtaposes the performance of both the proposed and contemporary models through various metrics. Section 5 concludes before the references are listed.

Table 1: Description of the formulas and acronyms

Medical IoT	Medical Internet of Things
ECG	Electro Cardiogram

BW	Baseline Wandering
PLI	Powerline Interference
WF	Weiner Filter
FT	Fourier-Transform
ASMF	Adaptive Switching Mean Filter
EMD	Empirical Mode Decomposition
NLM	Non-Local Mean
ENDQE	Electrocardiogram Noise Detection and Quality Estimation
ICU	Intensive Care Units
MCC	Max-Coefficient-Correlation
MFCC	Mel-Frequency-Cepstral-Coefficients
v_a, v_b	Vectors
$Ag(v_a), Ag(v_b)$	Aggregation
CR_{v_a}, CR_{v_b}	Cumulative Ratios
e_i	Element
pr	Previous Element in Reiteration
AD	The Absolute Distance
$p\tau$	Threshold Probability
WCs	Weak Classifiers
D_i	Distribution
$h_i : X \rightarrow \{-1, +1\}$	Hypothesis
P and N	Positive and Negative
tf_i	Temporal-Feature
SF	Spectral Feature
nG	N-grams
r_j	Record

2 Methods and Materials

The methods and associated materials used in the proposed model have been explored in this section. The methods used to fulfill the objectives of the learning phase, such as the method of selecting features and optimizing those features to reduce the process

complexity. The classifier trained by the corresponding optimal features and classifies the noise from the given electrocardiogram input is detailed in the following

subsections. Figure 1 represents the ENDQE block diagram.

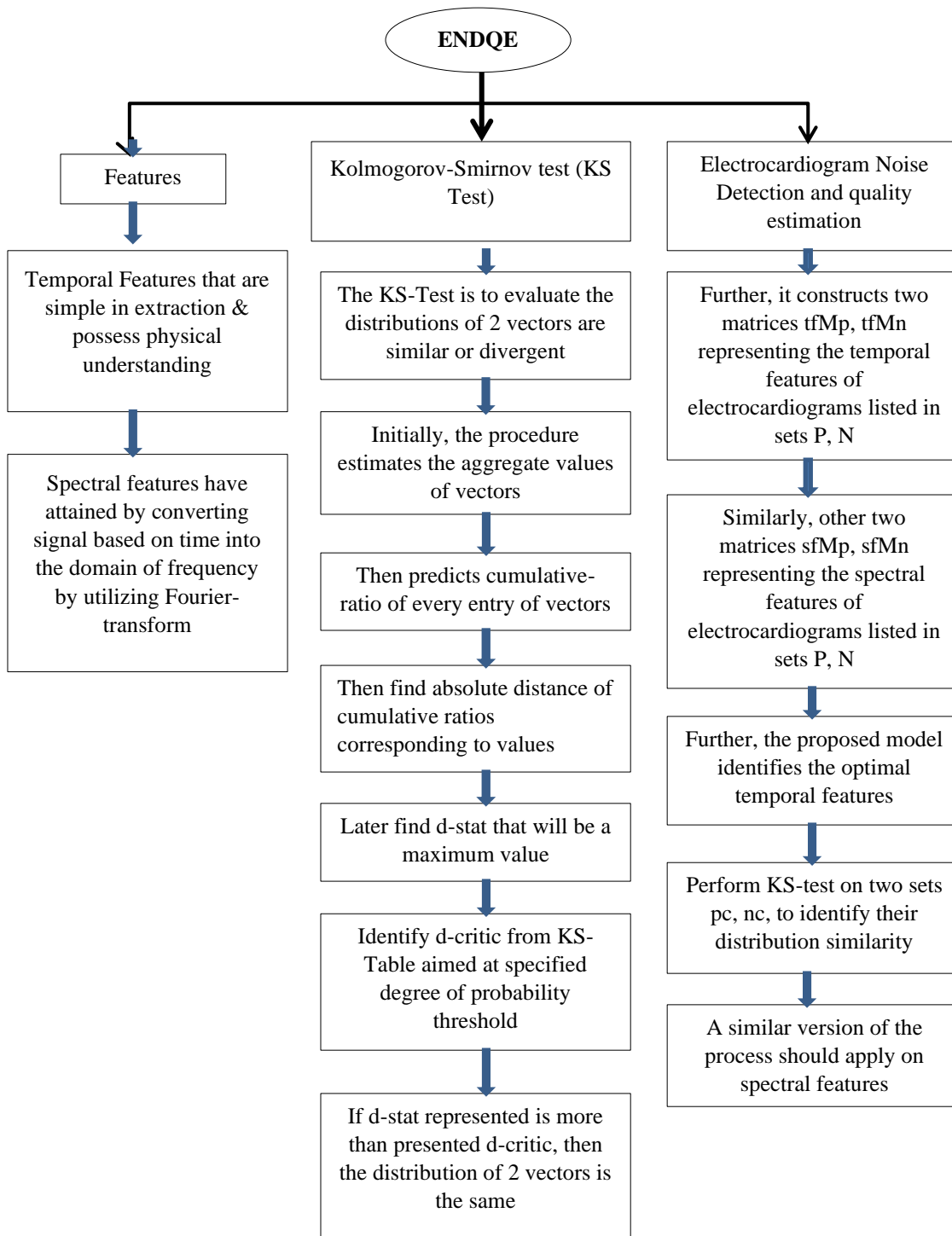


Fig 1: Block diagram representation of ENDQE

2.1 Features

The temporal features of the electrocardiogram signal feature such as energy, zero-rate of crossing shall be considered to explore the signal's physical structure. The spectral-related feature can be obtained by morphing the

signal of the time domain to the frequency domain. This phase of converting a signal from the time domain to the frequency domain can be done using Fourier transformation [17]. Further, the frequency domain's resultant signal shall be used as input to derive spectral

features such as frequency and its components, density, flux, roll-off, and the centroid of the corresponding spectrum. However, concerning the electrocardiograms, random variables to analyse noise spectrum evince complexity compared to electrocardiogram signals. A random spectrum with no information shall be considered to determine the spectral features from the signals' static noise [18]. The static noise does not have any special or unexpected occurrences. Hence, a significant variance can appear between static noise signals and signals of electrocardiograms. The Fourier transformation decomposes the electrocardiogram signal, which results in the spectral structure, diversified frequencies, and magnitudes. The prediction of noise is more robust if temporal features such as MCC (Max-coefficient-correlation), energy, index, and zero or null crossing rate (NCR or ZCR) are considered along with

spectral-domain features GTCC (Gammatone-cepstral-coefficients) and MFCC (Mel-Frequency-Cepstral-Coefficients).

2.2 Kolmogorov-Smirnov test (KS Test)

The KS test statistics reveal the gap between a cumulative and experimental sample distribution. Equal or diversified sizes of two experimental distribution samples can result in reported differences. A distance metric commonly known as KS-test or Kolmogorov-Smirnov test is used to show the distribution diversity state of the two datasets. Furthermore, this metric doesn't necessitate any data distribution details. As a de facto requirement, other distance metrics need this to estimate distribution diversity. The application process for the KS-test algorithmic approach is explained below:

ks_test(v_1, v_2) Begin //The input arguments v_a, v_b are two vectors.

Primarily, the process predicts the aggregation $Ag(v_a), Ag(v_b)$ of vectors v_a, v_b in respective order. Further, cumulative ratios are depicted in specified vectors v_a, v_b as corresponding sets CR_{v_a}, CR_{v_b} .

<pre> pr = 0 $\forall_{i=1}^{ v_j } \{e_i \exists e_i \in v_j\}$ begin pr = $\frac{e_i}{Ag(v_j)} + pr$ $CR_{v_j} \leftarrow pr$ end </pre>	<pre> // Finding the cumulative ratio for each vector's entry v_a, v_b has been predicted. the representation e_i indicates every element of a vector v_j, the representation pr indicates the accumulative ratio of the previous element in reiteration representation $Ag(v_j)$ indicates an aggregate of values represented in the v_j, the set CR_{v_j} incorporates cumulative ratios of overall elements that existed in v_j </pre>
---	---

Later identify the absolute cumulative ratios distance resulting in values, which are existed at an identical index of vectors v_a, v_b as stated below:

$\left. \begin{matrix} \max(CR_{v_a} , CR_{v_b}) \\ \forall_{i=1} \\ \left\{ \begin{matrix} c_i(v_a), c_i(v_b) \exists \\ c_i(v_a) \in CR_{v_a} \wedge c_i(v_b) \in CR_{v_b} \end{matrix} \right\} \end{matrix} \right\} \text{Begin}$	// for each i index, values existed in CR_{v_a}, CR_{v_b}
---	---

$AD_{CR_{v_a} \leftrightarrow CR_{v_b}} \leftarrow abs(c_i(v_a) - c_i(v_b))$ // represents the absolute distance of cumulative ratios AD presented in sets”
 CR_{v_a}, CR_{v_b} at the index and preserves in a set $AD_{CR_{v_a} \leftrightarrow CR_{v_b}}$.

End

Identify d-stat, which would be the highest value that is existed in

$AD_{CR_{v_a} \leftrightarrow CR_{v_b}}$

The d-critic aimed at KS-table has been identified for provided for the degree $Ag(v_a), Ag(v_b)$ of threshold

probability $p\tau$

If the d-stat depicted is greater than the d-critic presented, return 0//2 vectors are not distinct.

Else return 1 //two vector are distinct

End

2.3 The classifier

A group learning model known as Adaboost is mainly trained to enhance the efficacy of a binary classifier. In addition, Adaboost makes use of an iterative process to understand from subordinate classifiers' mistakes and transform them into influential errors. According to [20], the Adaboost classifier has created a reinforcing algorithm that adapts. The design of this classifier includes integration of branched Boolean classifiers, or weak classifiers (WCs). The data specified is partitioned into either false or true conditions by each weak classifier. False positives and negatives shall be distributed among the remaining WCs as part of negative. The negotiation by the entire WC to complete the challenge continues by repeating this action. The full integration of results obtained from these weak classifiers shall reflect in the ranking procedure's final result [21]. This article uses WC to represent the optimal characteristics that are consistent from the discrete class to the binary classification.

The classification procedure is iterative. For each iteration of the weak classifier, the central part, which failed to classify exactly, shall repeat the next classifier, which is often called the reinforcement. Here the Week Classifier, which is used for each iteration, shall be referred to by the rating weight. With the completion of iterative WC calls, WC-scored records shall be completely streamlined. Regarding the predicted method, Adaboost uses each WC, indicating a specific n-gram number to rank the accuracy. Besides, the WC classification results would streamline discovering the polarity of specific records against the proposed method [22]. For each feature class, a WC and the like would be involved, each class of the appropriate features would learn concerning both the noisy and qualified electrocardiograms. The mathematical model of the Adaboost classification is described the following. Eq 1.

$$\text{Given: } (x_1, y_1), \dots, (x_m, y_m) \text{ where } x_i \in X, \\ y_i \in \{-1, +1\} \quad (1)$$

Initialize: $D_1(i) = 1/m$ for $i = 1, \dots, m$

For $t = 1, \dots, T$

- Train weak learners using distribution D_t
- Get weak hypothesis $h_t : X \rightarrow \{-1, +1\}$

- Aim: select h_t with low weighted error

$$\varepsilon_t = \Pr_{i \sim D_t} [h_t(x_i) \neq y_i] \quad (2)$$

- Choose $\alpha_t = \frac{1}{2} \ln \left(\frac{1 - \varepsilon_t}{\varepsilon_t} \right)$

- Update, for $i = 1, \dots, m$

$$D_{t+1}(i) = \frac{D_t(i) \exp(-\alpha_t y_i h_t(x_i))}{Z_t} \quad (3)$$

Where Z_t is a normalization factor (chosen so that D_{t+1} will be a distribution)

Output the final hypothesis:

$$H(x) = \text{Sign} \left(\sum_{t=1}^T \alpha_t h_t(x) \right) \quad (4)$$

2.4 Electrocardiogram Noise Detection and Quality Estimation

Two groups P, N must be created for the set of electrocardiograms given. The two groups of recordings P are recognized as positive and N negative based on whether they represent a valid ECG or a noisy one, respectively. In their respective order, two tables representing the temporal characteristics of electrocardiograms are constructed by the proposed model as groups P, N . The other two tables $sfMp, sfMn$ display the electrocardiograms' spectral characteristics listed in groups, as well. The optimal time traits are recognized as follows in Equation. 5:

$$\bigvee_{i=1}^{|tfMp|} \{pc_i, nc_i, \exists pc_i \in tfMp \wedge nc_i \in tfMn\} \quad (5)$$

// Iterates until all the columns of both tables are processed, considering the column pc_i from the table $tfMp$ and the column nc_i from the table $tfMn$ as inputs to KS-test

The function $ks-test(pc_i, nc_i)$ invokes the vectors pc_i, nc_i as input parameters, which predicts the diversity between these two vectors. If diversity is found between these vectors, then the temporal-feature tf_i

representing these vectors shall be considered optimal[24]. If not (no diversity found), then the feature tf_i is suboptimal. Hence discard the corresponding vectors pc_i, nc_i from the respective sets $tfMp, tfMn$.

After completion of the iterations in equation 5, the tables $tfMp, tfMn$ retain values for optimal features. A similar version of the process shall apply to the spectral feature tables $sfMp, sfMn$, which results in the optimal spectral features[25]. The different phase discovers the

optimal n-gram features for both the labels, as explored in the following section.

2.5 Discovering n-gram features

By inputting the features corresponding to the columns in resultant sets $tfMp, tfMn, sfMp, sfMn$ one can obtain all possible unique subsets. The n-gram features are represented in subsequent descriptions through these subsets. Discovering n-grams of changing sizes is explored through a mathematical model in the subsequent explanation.

$n - gram_features(aL)$

Begin

$nGr \leftarrow aL$

The set aL is the default set of 1-grams. Hence, the attributes listed in the set aL shall move to the set nG of n-grams

$tnG \leftarrow nGr$

The set tnG is the clone of the set nGr

$while(|tnG| > 0)$ Begin

While the set tnG is not empty

$\forall_{i=1}^{|tnG|} \{ng_i, \exists ng_i \in tnG\}$

For each n-gram ng_i of the set tnG

Begin

$\forall_{j=1}^{|tnG|} \{ng_j, \exists ng_j \in tnG \wedge i \neq j\}$

For each n-gram ng_j of the set tnG that does not equal to the n-gram ng_i

Begin

$ng \leftarrow \{ng_i \cup ng_j\}$

New n-gram ng , which is the union of two n-grams ng_i, ng_j that denotes

$if(ng \notin nGr)$

$nGr \leftarrow ng$ If n-gram ng does not exist in the set nGr of n-grams, add n-gram ng to the set nGr

End

// of the loop $\forall_{j=1}^{|tnG|} \{ng_j, \exists ng_j \in tnG \wedge i \neq j\}$

End

// of the loop $\forall_{i=1}^{|tnG|} \{ng_i, \exists ng_i \in tnG\}$

$if(|nGr| > |tnG|)$ Begin

If the size $|nGr|$ of the set nGr is greater than the size $|tnG|$

$tnG \setminus nGr$

Empty the set tnG

$tnG \leftarrow nGr$

Add all the n-grams of the set nGr to the empty set tnG

End

of the condition $if(|nGr| > |tnG|)$

$elseif(|nGr| \equiv |tnG|)$

If both the sets nGr, tnG having the same size, empty the set tnG

End

// of the loop $while(|tnG| > 0)$

The resultant set nGr contains all possible subsets of attributes (column labels) of the set aL . The further phase of the proposed method discovers the n-gram feature values and their confidence towards both sets tD_+, tD_- as follows

$\forall_{i=1}^{|nGr|} \{ng_i, \exists ng_i \in nGr\}$ Begin

// for each n-gram ng_i feature of the set nGr

$fv(ng_i)$ // is an empty set that contains unique n-grams of feature values of the n-gram feature ng_i , both positive and negative labels

$\forall_{j=1}^{|tD_+|} \{r_j \exists r_j \in tD_+\}$ Begin // for each record r_j of the set tD_+

$fv(ng_i) \leftarrow \{v(ng_i) \exists v(ng_i) \subseteq r_j \wedge v(ng_i) \notin fv(ng_i)\}$ values $v(ng_i)$ that are a subset of record r_j of the positive label and do not exist in the set $fv(ng_i)$ of the n-gram feature ng_i

End // of the loop $\forall_{j=1}^{|tD_+|} \{r_j \exists r_j \in tD_+\}$

$\forall_{j=1}^{|tD_-|} \{r_j \exists r_j \in tD_-\}$ Begin // for each record r_j of the set tD_- of records labeled as negative

$fv(ng_i) \leftarrow \{v(ng_i) \exists v(ng_i) \subseteq r_j \wedge v(ng_i) \notin fv(ng_i)\}$ values $v(ng_i)$ that are a subset of record r_j of the negative label and do not exist in the set $fv(ng_i)$ of the n-gram feature ng_i

End // of the loop $\forall_{j=1}^{|tD_-|} \{r_j \exists r_j \in tD_-\}$

End // of the loop $\forall_{i=1}^{|nGr|} \{ng_i \exists ng_i \in nGr\}$

#Finding the positive and negative confidence of each n-gram feature values#

$\forall_{i=1}^{|nGr|} \{ng_i \exists ng_i \in nGr\}$ Begin // for each n-gram ng_i feature of the set nGr

$\forall_{j=1}^{|fv(ng_i)|} \{v_j \exists v_j \in fv(ng_i)\}$ Each n-gram feature value v_j of the n-gram feature ng_i

$pc_+ \leftarrow \frac{1}{|tD_+|} \left(\sum_{k=1}^{|tD_+|} \{1 \exists v_j \subseteq r_k\} \right)$ Move positive confidence of n-gram feature value v_j

$pc_- \leftarrow \frac{1}{|tD_-|} \left(\sum_{k=1}^{|tD_-|} \{1 \exists v_j \subseteq r_k\} \right)$ Move negative confidence of n-gram feature value v_j

End // of the loop $\forall_{j=1}^{|fv(ng_i)|} \{v_j \exists v_j \in fv(ng_i)\}$

End // of the loop $\forall_{i=1}^{|nGr|} \{ng_i \exists ng_i \in nGr\}$

The resultant n-gram features of both temporal and spectral formats shall be used to train the classifier that classifies the given electrocardiogram is noisy or not.

3 Experimental Study

The experimental research was conducted to highlight the importance of ENDQE, the proposed method. Performing cross-validation of the proposed method ENDQE and the contemporary model 'Denosing of

Electrocardiogram (ECG) Signal by Using Empirical Mode Decomposition (EMD) with Non-local Mean (NLM) Technique (EMD+NLM)' [16] was done using the benchmark dataset MIT-BIH [23]. Both methods have compared and scaled the performance of the proposed model, ENDQE, using the resultant cross-validation metric values. The number of records in the adopted corpus of electrocardiograms is 14423. This set includes both qualified (7802) as well as noisy (6621)

electrocardiograms. Tenfold cross-validation has been performed on the dataset having both qualified and noisy electrocardiograms. Concerning tenfold cross-validation, the dataset of both labels was partitioned to 10 equal shares. On each fold of the cross-validation, one share of

the dataset has been used for testing, and the rest nine shares have been used for training.

3.1 The Performance Analysis

The cross-validation metric values have compared and analyzed the performance Table 2

Table 2: values obtained for cross-validation metrics from ENDQE and EMD+NLM methods

FOLD ID#	1	2	3	4	5	6	7	8	9	10
PRECISION										
ENDQE	0.9062	0.8743	0.8812	0.8853	0.9023	0.884	0.8756	0.886	0.8827	0.8868
EMD+NLM	0.8406	0.8364	0.8676	0.8508	0.8553	0.8792	0.8839	0.8729	0.8612	0.8679
SENSITIVITY										
ENDQE	0.9405	0.9535	0.9599	0.9503	0.9474	0.9579	0.9563	0.9567	0.9553	0.9544
EMD+NLM	0.9194	0.9376	0.9159	0.928	0.9472	0.9338	0.9271	0.9239	0.9306	0.9263
SPECIFICITY										
ENDQE	0.9522	0.9321	0.9358	0.9395	0.9495	0.9381	0.9332	0.9391	0.9373	0.9398
EMD+NLM	0.9137	0.9092	0.9307	0.9199	0.921	0.9365	0.9398	0.9338	0.9258	0.9304
ACCURACY										
ENDQE	0.9483	0.9394	0.9441	0.9428	0.9487	0.9445	0.9407	0.9449	0.9432	0.9445
EMD+NLM	0.9157	0.9186	0.9258	0.9225	0.9297	0.9356	0.9356	0.9305	0.9275	0.9292
F-MEASURE										
ENDQE	0.9286	0.9023	0.9077	0.9116	0.9253	0.9102	0.9035	0.9118	0.9092	0.9125
EMD+NLM	0.8756	0.8713	0.898	0.884	0.8869	0.9069	0.911	0.9023	0.8923	0.8981
MATHEWS CORRELATION COEFFICIENT										
ENDQE	0.8847	0.8681	0.8783	0.8743	0.8862	0.8788	0.871	0.8795	0.8759	0.8783
EMD+NLM	0.8158	0.8248	0.8354	0.8306	0.8479	0.8576	0.8568	0.8461	0.841	0.8439

The results obtained for cross-validation metrics report the performance significance of the proposed method ENDQE over the contemporary method EMD+NLM. Metric level details have been explored in the following description. The value gained from those trained through cross-validation on both methods is known as the precision metric: 0.88640.0098 (89%) and

0.861580.014976502 (86.5%), for ENDQE and EMD+NLM, respectively. Figure 2 showcases the precision details observed in each fold of the cross-validation. In terms of metric precision, the significance of ENDQE is reported with minimal deviation compared to the contemporary model EMD+NLM.

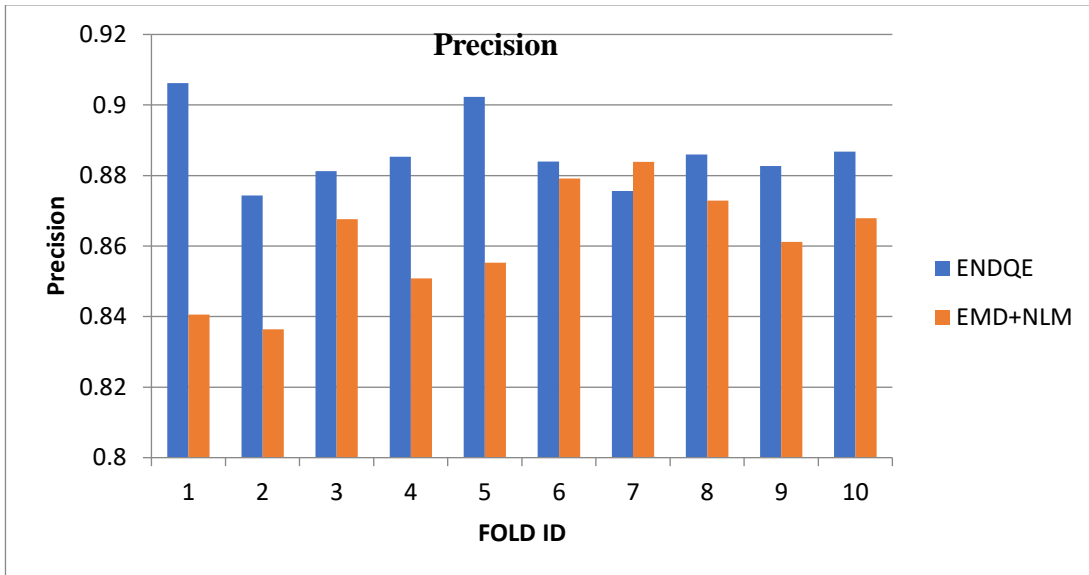


Fig 2: The positive predictive values observed from cross-validation

The True Negative Rate that refers to specificity observed for both ENDQE and EMD+NLM methods are 0.9397 ± 0.0061 (94%), and 0.9261 ± 0.0095 (93%) from tenfold cross-validation. The specificity observed from each fold of the cross-validation has been briefed in

Figure 3. The values obtained for metric specificity report the significance of the ENDQE with minimal deviation compared to the contemporary model EMD+NLM.

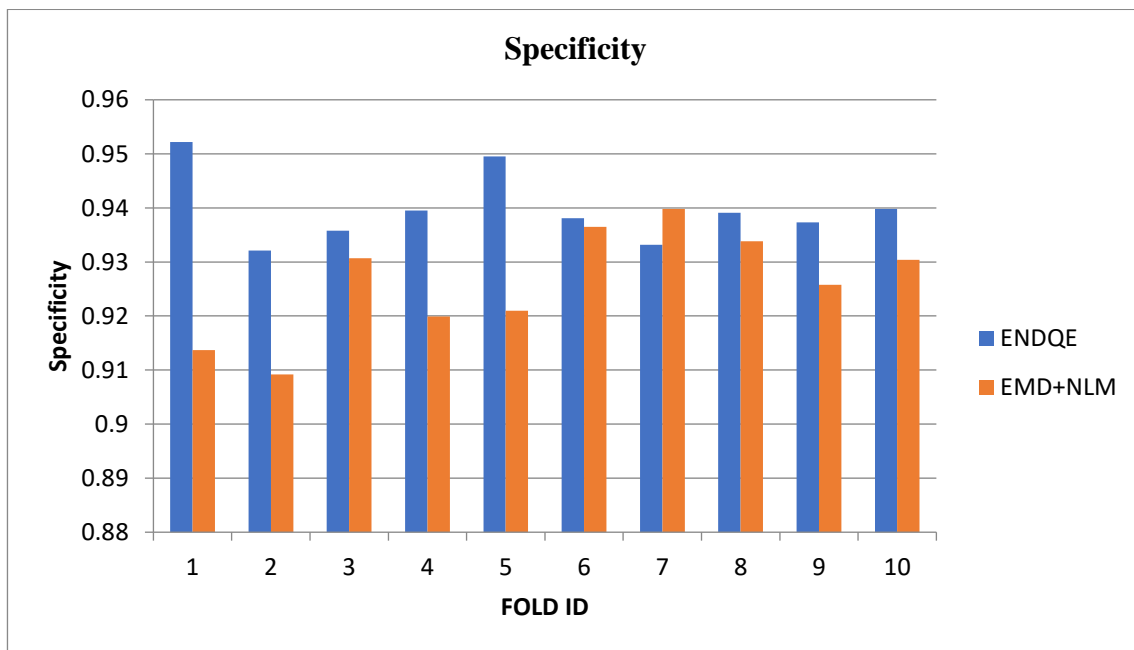


Fig 3: The True Negative Rate obtained from cross-validation

The true positive rate also refers to sensitivity observed from cross-validation performed on both methods ENDQE, EMD+NLM are 0.9532 ± 0.00546 (95%), and 0.9290 ± 0.0086 (93%) in respective order. The details of

the fold level sensitivity have been figured in Figure 4. The values obtained for metric sensitivity reporting the significance of the ENDQE with better performance when compared to the contemporary model EMD+NLM.

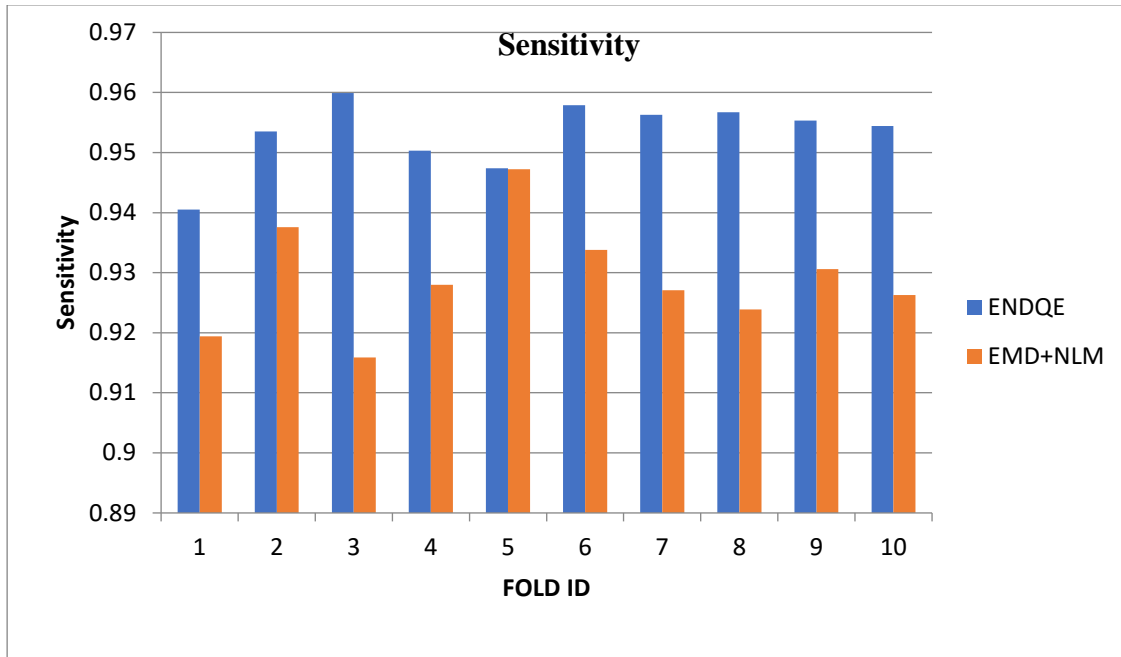


Fig 4: the sensitivity observed from tenfold cross-validation

The cross-validation metric “prediction accuracy” denotes the ratio of correctly labeled records against the total number of records. The overall prediction accuracy observed for ENDQE and EMD+NLM is 0.9441 ± 0.0028 (95%) and 0.92707 ± 0.0063 (93%). The detailed

statistics of accuracy obtained from tenfold cross-validation have been explored in Figure 5. The values obtained for metric Accuracy reporting the significance of the ENDQE with better performance while compared to the contemporary model EMD+NLM.

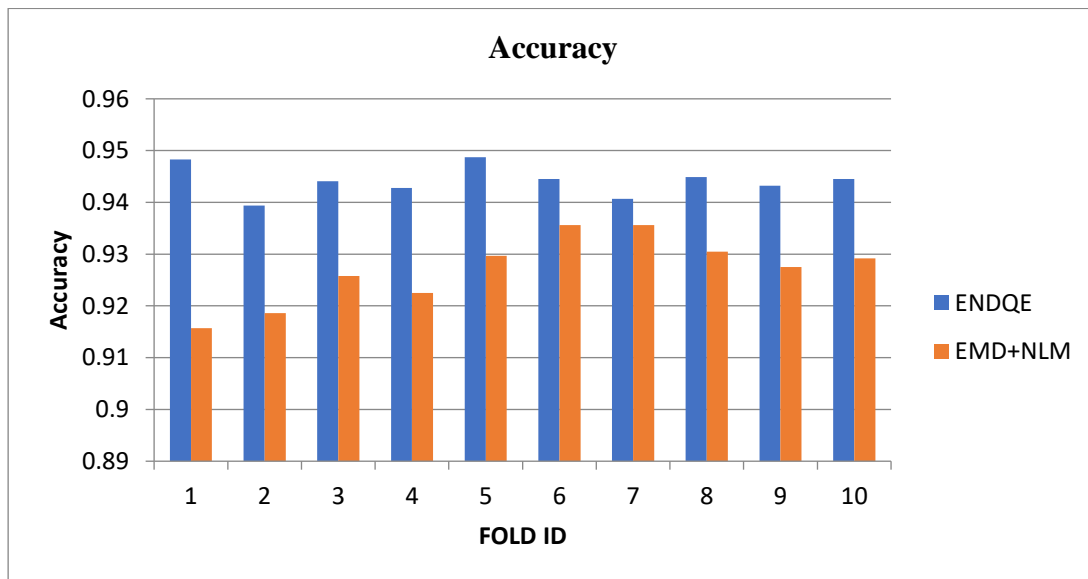


Fig 5: Accuracy obtained from tenfold cross-validation

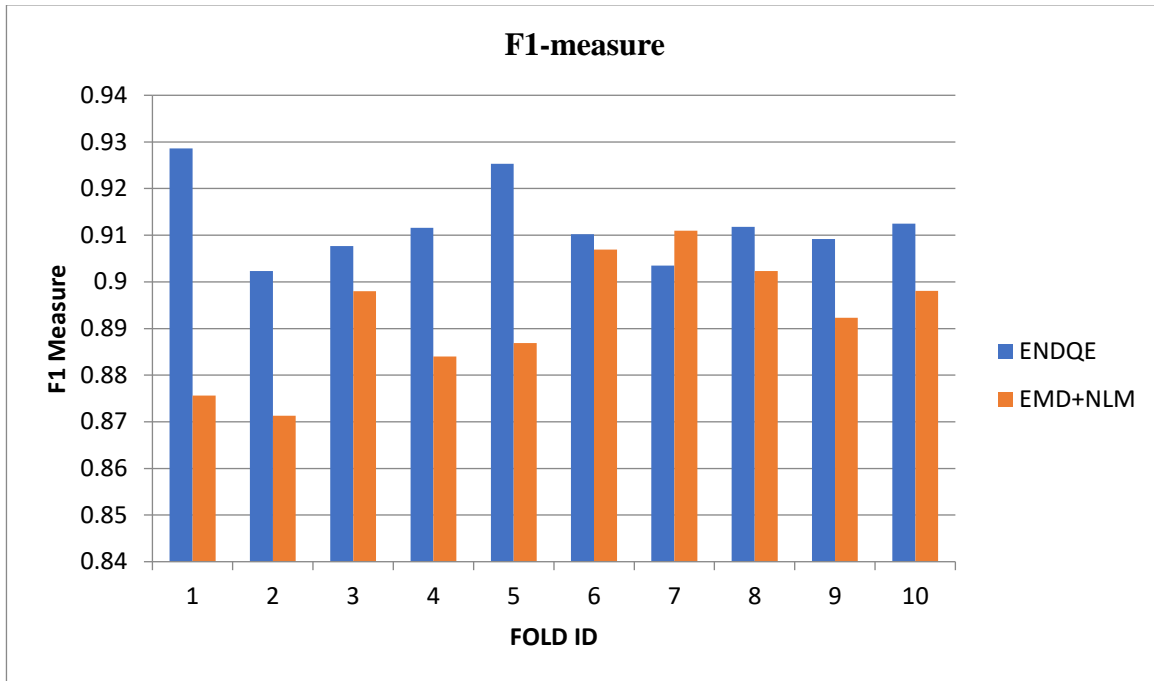


Fig 6: The f-measure observations from tenfold cross-validation

The cross-validation metric “F-measure” has been measured over the proposed and contemporary models among ten folds, as shown in figure 6. The average f-measure depicted for ENDQE and EMD+NLM are 0.91 ± 0.008 (91%) and 0.8926 ± 0.012 (89%) in respective

order. The detailed statistics of F-measure obtained from tenfold cross-validation have been explored in Figure 6. The values obtained for metric f-measure exhibit the significance of the ENDQE with better performance while compared to the contemporary model EMD+NLM.

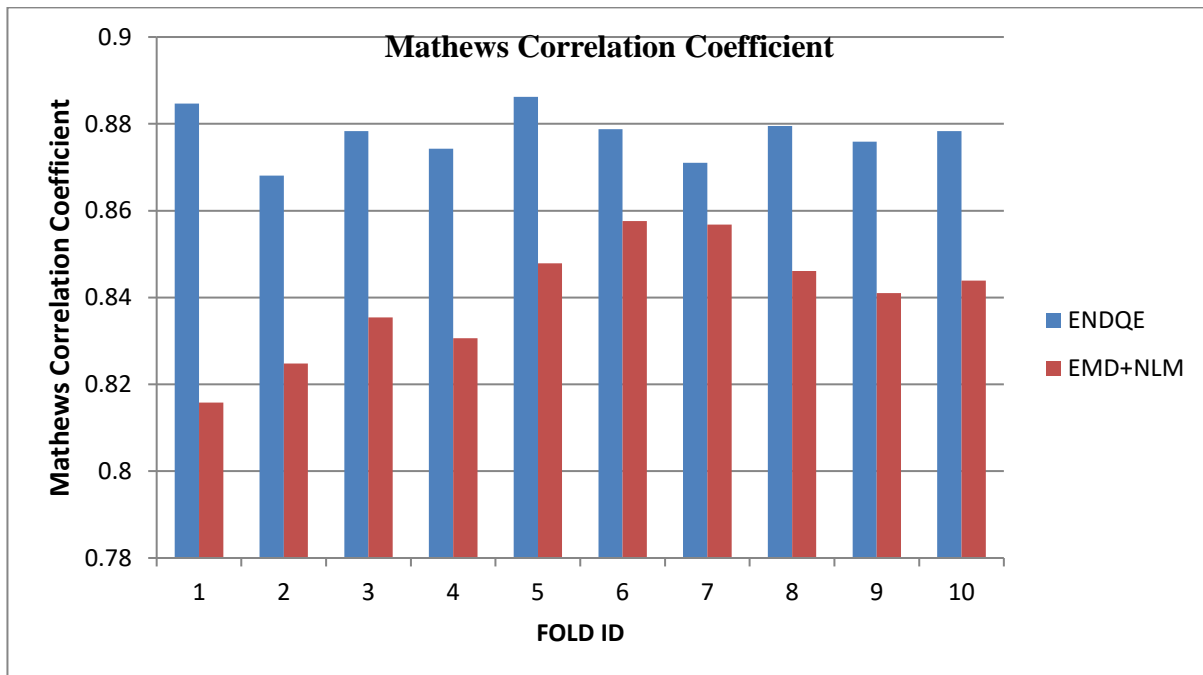


Fig 7: The Mathews Correlation Coefficient (MCC) observed from the tenfold cross-validation

The cross-validation metric MCC has been measured over the proposed and contemporary models among ten folds, as shown in Figure 7. The MCC observed for ENDQE and EMD+NLM are $0.8780.005$ (89%) and $0.840.013$ (84%) in the respective order. The detailed statistics of MCC obtained from tenfold cross-validation have been explored in Figure 7. The values obtained for

metric MCC exhibits the significance of the ENDQE with better performance while compared to the contemporary model EMD+NLM.

4 Conclusion

This paper proposes a novel approach that classifies the given input electrocardiograms as qualified or noisy,

which reduces the false alarm in machine learning-based arrhythmia detection. The noise localization has been optimized through the classification process that learns from the optimal temporal and spectral features selected by a KS-Test distribution diversity measure. The classification process has been done by using the Adaboost technique trained by the selected optimal features. The accuracy in discriminating the qualified and noisy electrocardiograms is considerably significant from the proposed method. The contemporary measure called “empirical mode decomposition with the non-local mean for denoising the electrocardiogram signals” has been used to scale the proposed method’s performance. However, the work is limited to identifying the noise scope in electrocardiograms. Future research shall intend to remove noise from electrocardiograms using soft-computing measures. The other future research dimension shall use wavelet parameters to identify the weak noise signals from the electrocardiograms.

References

- [1] Kumar, A. (2010). ECG-simplified. LifeHugger. (2010) Nov. <http://pn.lifehugger.com/doc/120/ecg-100-steps>
- [2] Lilly, L. S. (2012). Braunwald’s heart disease: a textbook of cardiovascular medicine. Elsevier Health Sciences, vol. 2. Medico-legal Update, <https://www.ijop.net/index.php/mlu/article/download/2535/2231>
- [3] Wu, J. M.-T. (2020). A deep neural network electrocardiogram analysis framework for left ventricular hypertrophy prediction. *Journal of Ambient Intelligence and Humanized Computing*, 1-17, <https://doi.org/10.1007/s12652-020-01826-1>.
- [4] P, P., & J, K. (2023). Effective Predictor Model for Parkinson’s Disease Using Machine Learning. *International Journal of Computer Engineering in Research Trends*, 10(4), 204–209. <https://doi.org/10.22362/ijcert.v10i4.27>
- [5] Care, I. E. (2005). Part 8: Stabilization of the patient with acute coronary syndromes. *Circulation*, IV-90-IV-110. <https://doi.org/10.1161/CIRCULATIONAHA.105.166561>
- [6] Hongqiang Li, Danyang Yuan, Youxi Wang, Dianyin Cui, Lu Cao (2016). Arrhythmia classification based on multi-domain feature extraction for an ECG recognition system. *Sensors*, 16(10), 1744. DOI: 10.3390/s16101744
- [7] G, P., S, R., & Bedhapuri, M. (2023). Next-Generation Eye Care: IoT-Driven Disease Detection and Emergency Alerts using DL. *International Journal of Computer Engineering in Research Trends*, 9(3), 66–76. <https://doi.org/10.22362/ijcert.v9i3.30>
- [8] Rehman, U. a. (2014). Noise Removal From ECG Using Modified CSLMS Algorithm. *International Journal of Electronics, Communication & Instrumentation Engineering Research & Development*, 4(3), 53-60. www.tjprc.org
- [9] M. Rudra Kumar, V. K. (2020). Review of Machine Learning models for Credit Scoring Analysis. *Revista Ingeniería Solidaria*, 16(1). <https://doi.org/10.16925/2357-6014.2020.01.11>
- [10] Boge, A. V. (2012). Clearing Artifacts using a Constrained Stability Least Mean Square Algorithm from Cardiac Signals. *International Journal of Scientific & Engineering Research*, 3(11), 1-6. <http://www.ijser.org>
- [11] Kim, J.-C. a. (2020). Neural-network based adaptive context prediction model for ambient intelligence. *Journal of Ambient Intelligence and Humanized Computing*, 11(4), 1451-1458. <https://doi.org/10.1007/s12652-018-0972-3>
- [12] Gayatri Khanvilkar, Deepali Vora (2018). Activation Functions and Training Algorithms for Deep Neural Network. *International Journal of Computer Engineering in Research Trends*, 5(4),98-104.
- [13] Joao Rodrigues, David Belo, Hugo Gamboa (2017). Noise detection on ECG based on agglomerative clustering of morphological features. *Computers in biology and medicine*, 87, 322-334. DOI: 10.1016/j.combiomed.2017.06.009
- [14] Haemwaan Sivaraks, Chotirat Ann Ratanamahatana (2015). Robust and accurate anomaly detection in ECG artifacts using time series motif discovery. *Computational and mathematical methods in medicine*, vol. 2015, pp. 1-20, <https://doi.org/10.1155/2015/453214>.
- [15] Udit Satija, Barathram Ramkumar, M Sabarimalai Manikandan (2017). Automated ECG noise detection and classification system for unsupervised healthcare monitoring. *IEEE Journal of biomedical and health informatics*, 22(3), 722-732. DOI: 10.1109/JBHI.2017.2686436
- [16] Kumar.S, Panigrahy.D, Sahu.P.K. (2018). Denoising of Electrocardiogram (ECG) signal by using empirical mode decomposition (EMD) with non-local mean (NLM) technique. *Biocybernetics and Biomedical Engineering*, 38(2), 297-312.

- [17] Gummadi, A. ., & Rao, K. R. . (2023). EECLA: A Novel Clustering Model for Improvement of Localization and Energy Efficient Routing Protocols in Vehicle Tracking Using Wireless Sensor Networks. *International Journal on Recent and Innovation Trends in Computing and Communication*, 11(2s), 188–197. <https://doi.org/10.17762/ijritcc.v11i2s.6044>
- [18] Neha Agrawal, Shashikala Tapaswi (2018). Low rate cloud DDoS attack defense method based on power spectral density analysis. *Information Processing Letters*, 138, 44-50. <https://doi.org/10.1016/j.ipl.2018.06.001>
- [19] Gautier Marti, Frank Nielsen, Mikołaj Bińkowski, Philippe Donnat (2017). A review of two decades of correlations, hierarchies, networks and clustering in financial markets. arXiv preprint arXiv:1703.00485. <https://doi.org/10.48550/arXiv.1703.00485>
- [20] Asghar Ghasemi, Saleh Zahediasl (2012). Normality tests for statistical analysis: a guide for non-statisticians. *International journal of endocrinology and metabolism*, 10(2), 486. doi: 10.5812/ijem.3505
- [21] Tae-Ki An, Moon-Hyun Kim (2010). A new diverse AdaBoost classifier. 2010 International Conference on Artificial Intelligence and Computational Intelligence, 1, 359-363. DOI:10.1109/AICI.2010.82
- [22] Benedetto Barabino, Nicola Aldo Cabras, Claudio Conversano & Alessandro Olivo (2020). An integrated approach to select key quality indicators in transit services. *Social Indicators Research*, 1-36. DOI: 10.1007/s11205-020-02284-0
- [23] S Celin & K. Vasanth (2018). ECG signal classification using various machine learning techniques. *Journal of medical systems*, 42(12), 1-11. <https://doi.org/10.1007/s10916-018-1083-6>
- [24] Sherje, D. N. . (2021). Content Based Image Retrieval Based on Feature Extraction and Classification Using Deep Learning Techniques. *Research Journal of Computer Systems and Engineering*, 2(1), 16:22. Retrieved from <https://technicaljournals.org/RJCSE/index.php/journal/article/view/14>
- [25] Moody GB, M. R. (2001). The impact of the MIT-BIH arrhythmia database. *IEEE Engineering in Medicine and Biology Magazine*, 20(3), 45-50.
- [26] S. Sandhya kumari , K.Sandhya Rani (2022). Selection of MSER region based Ultrasound Doppler scan Image Big data classification using a faster RCNN network. *International Journal of Computer Engineering in Research Trends*.9(10),184-192.